REVIEW

Glass ceramic ZERODUR®: Even closer to zero thermal expansion: a review, part 2

Peter Hartmann,* Ralf Jedamzik, Antoine Carré, Janina Krieg, and Thomas Westerhoff
Schott AG, Mainz, Germany

Abstract. Observational astronomy has sought better telescopes with higher resolution from its beginning. This needs ever-larger mirrors with stable, high-precision surfaces. The extremely low-expansion glass ceramic ZERODUR® has enabled such mirrors for more than 50 years with significant improvements in size and quality since then. We provide a survey of the progress achieved in the last 15 years. Equally important as the thermal expansion coefficient CTE is its homogeneity. The CTE variation in 4-m mirror blanks lies below 5 ppb/K in radial and axial directions on large and short scales. Improved measurement capabilities allow reduced bias, which in the past made variations look greater than they were. Isotropy and uniformity of ZERODUR are outstanding. A method for lifetime calculation increases reliability considerably with respect to mechanical loads. The production and metrology capability and capacity are greatly extended. Surface figure and texture of large blanks allow starting directly with polishing. Filigree structures with up to 90% weight reduction are well-suited for space mirrors. The progress with low thermal expansion and its measurement, the insensitivity of ZERODUR against ionizing radiation in space, and outstanding application examples are presented in the first part of our review. [DOI: 10.1117/1.JATIS.7.2.020902]

Keywords: ZERODUR®; extremely low expansion; glass ceramic; coefficient of thermal expansion; homogeneity; large size; monolithic; lightweighting.

Paper 20170V received Nov. 24, 2020; accepted for publication May 3, 2021; published online Jun. 3, 2021.

1 Introduction

Fifty years after its introduction, one could expect that all properties of a material are explored and well known. However, in the case of the extremely low-thermal-expansion glass ceramic ZERODUR®, the story turned out differently. As soon as the material was introduced into application, users began challenging its properties and quality standards. New projects in science and technology keep on pushing the key requirement of preserving shape and dimensions with utmost precision within varying temperature fields. Admissible tolerances travel down the length scale from microns to nanometers and even picometers for larger and larger mirrors and structures. ZERODUR revealed its potential to follow this development to an extent that even 15 years ago no one would have expected. The progress is not restricted to only one property. It covers a wide range including the key property of low thermal expansion as well as homogeneity, radiation resistance, mechanical strength, and workability to large mirrors and other large, lightweight structures.

As a glass ceramic, ZERODUR is a material between both extremes of glass and crystal, either of which are free from the opposite configuration. A glass ceramic consists of a combination of a glassy phase and a crystalline phase. A tempering process allows creation of nanometer-sized crystals within a pure glass, which are interspersed homogenously throughout the total volume. With lithium-aluminum-silicate glass ceramics such as ZERODUR, the nanocrystals provide a negative thermal expansion. A finely balanced mixture of the crystal phase and the residual glass will lead to a net thermal expansion very close to zero. Control parameters are

*Address all correspondence to Peter Hartmann, peterhartmann17@gmail.com; peter1.hartmann@schott.com

crystal size and number per volume. For more and detailed information, refer to the book of H. Bach (Ed.) on low thermal expansion glass ceramics.[1]

Melting, casting, and precision tempering especially of large ZERODUR items benefits strongly from Schott's long-time experience gained from optical glass production. Therefore, many outstanding properties of optical glass can be found in ZERODUR: the very high controllability of the absolute value and the outstanding homogeneity of its key property. For optical glass, this is the index of refraction, and for ZERODUR it is low thermal expansion. Further parallels are their very high internal material quality (low bubble and inclusion, striae, and stress content) and the capability to produce large (meter-sized) items. Only the combination of all these aspects and the capability to achieve such quality with high reproducibility enabled the material to find very successful applications in astronomical telescopes and in high-tech industry.[2,3]

Since 2005, roughly speaking, further progress led to astonishing improvements in several aspects of high importance for leading edge applications.

First, the key property of low expansion could be restricted even closer to zero leading to narrower tolerances for the coefficient of thermal expansion (CTE). Moreover, a method that allows adapting specific batches to the temperature profile prevailing in specific applications enables a further reduction of the expansion by a factor up to 10 with respect to the lowest value possible before. The denomination of the corresponding quality grade is ZERODUR Tailored.

Second, the improved expansion homogeneity now lies within the single-digit ppb/K (parts per billion per Kelvin) range. This holds true for short distances of centimeters as well as up to 4 m in diameter in radial and in axial directions. Dilatometers with improved statistical reproducibility allowed proving this.

Third, developments in mechanical grinding allow production of structures with a rib thickness of only 2 mm to yield 200 mm in height, enabling mirrors with a weight reduction close to 90%. Generating such structures from a cast item removes any doubts about integrity which are common with structures made by joining elements.

Fourth, extensive research on the mechanical strength of ZERODUR has shown that it is suitable for applications with much higher bending stress loads than thought before and that the minimum lifetime of loaded structures can be calculated reliably. Finally, a meta-study has proven a much higher resistance of ZERODUR against radioactive environment which is subject to confirmation by ongoing further research.

Due to the plethora of available information, this paper comes in two parts. The first part concentrates on the low thermal expansion under ambient conditions and within the cryo temperature range, the expansion measurement methods used, long-term stability, and the resistance against ionizing radiation as encountered in space applications. The second part highlights the homogeneity of the thermal expansion and the material homogeneity, the mechanical strength and progress in manufacturing technology of extremely lightweighted mirror blanks, or large 4-m mirror blanks ready for polishing

2 CTE Homogeneity of ZERODUR Blanks up to 8 M in Diameter

2.1 *Importance of CTE Homogeneity*

The homogeneity of the CTE across the volume of astronomical mirrors is of equal importance as its extremely low value. In some application cases, it is valued even higher. Some residual expansion might be acceptable if it is uniform and when measures exist allowing compensation. Varying expansion in different parts of the volume, however, is hard to compensate. In most cases, it is just impossible, and warping becomes fully effective, distorting the image quality. For this reason, the requirement of very low variation of the CTE throughout the total mirror volume was set from the very beginning of ZERODUR production. The larger the size of the mirrors grew, the more prominent became the requirement, and the more challenging the methods to fulfill and prove it.[4,5]

Achieving near-zero expansion with a glass ceramic needs a delicate control of the nanocrystals' size and number per volume. It is achieved by exposing the still glassy material to a

well-defined temperature time program comprising two essential steps. The first step serves for creating crystal nuclei and the second step for controlling their growth up to the required size. This precise temperature time program must be equal for all partial volumes throughout the total volume of the mirror blank. Any differences will result in permanent local differences in CTE and thus in poor homogeneity.

The challenge is to keep temperature–time courses equal within all partial volumes of a glass or glass-ceramic. Due to their very low thermal conductivity, high-temperature gradients occur in the volume with rapid temperature changes. Unfortunately, the gradients rise non-linear with material thickness. For flat extended items, they follow roughly the square of the thickness. The only way to avoid critical gradients is to make the temperature–time programs very slow. For this reason, thick ZERODUR mirror blanks remain in furnaces for up to 1 year. In principle, this is very similar to precision tempering processes used for large optical glass lenses in order to achieve high-refractive index homogeneity. The experience Schott gained since the end of the 19th century in producing large lenses was a great starting help for achieving the outstanding ZERODUR CTE homogeneity of today.

Another presupposition for extreme homogeneity roots also in the optical glass heritage: the melting and casting capability for highly homogeneous material. This means very low local variation in chemical composition and the absence of striae and of inclusions of alien materials. Preparation of very pure and homogenous raw material, melting, homogenization of the melt, and preservation of homogeneity during casting are process steps that had been already optimized for optical glass. Impressive demonstrations show that the technology transfer has worked. Interferometric measurements of ZERODUR disks have shown refractive index homogeneity with variations in the sixth decimal place, just as with the best optical glass. It is not surprising that CTE varies also with such extremely minute amounts.

However, simple size upscaling alone is not sufficient for mastering homogeneity. For ZERODUR, it needed extensive process development. The required sizes and thus cast volumes are much larger than those of optical glass. The largest cast optical glass disks weighed up to 500 kg, whereas ZERODUR 8-m raw blanks reached a weight of 45 tons.

2.2 *CTE Homogeneity Measurement*

CTE homogeneity is defined as the peak-to-valley difference of the CTE within the total volume of a given piece of material. In principle, this requires measuring CTE throughout the total volume in lateral and in vertical directions at best with a non-destructive method of extreme precision. Unfortunately, such a non-destructive method is not available for ZERODUR. Specific material samples have to be extracted from the piece to be measured using a push-rod dilatometer. The samples have to be of a minimum length in order to obtain detectable length changes while changing temperature in a reasonable interval. The sample length used by Schott is 100 mm and its diameter is 6 mm. In order to obtain a CTE reproducibility of 0.5 ppb/K, the length change of 3 nm has to be detected reliably within the temperature interval of 50°C. This is the reproducibility value Schott achieved with their advanced dilatometer (see part 1 of this paper).[6]

Figure 1 shows an example of the distribution of measurement samples (MP) that are taken from the raw glass-ceramic blank providing sufficient dimensional surplus. Usually, several samples will be taken from the centers of the top and bottom planes, their outer diameters, and if necessary, from diameters in between. For thick pieces, additional samples are taken from the outer diameter at half the height of the blank. In any case, homogeneity determination relies on a set of CTE measurements of samples extracted at different locations. This raises the questions, how representative and how accurate are the results?

2.3 *CTE Homogeneity Achieved in Practice*

Schott has reported repeatedly on the CTE homogeneity of ZERODUR blanks of all kinds of shapes and dimensions.[7–10] Table 1 provides a list of the CTE properties achieved with 4-m class blanks delivered by Schott since 2003.

This table shows a significant drop in the CTE homogeneity values from the two 4-m blanks delivered in 2003 and in 2005 to those delivered later. There are two reasons for this progress.

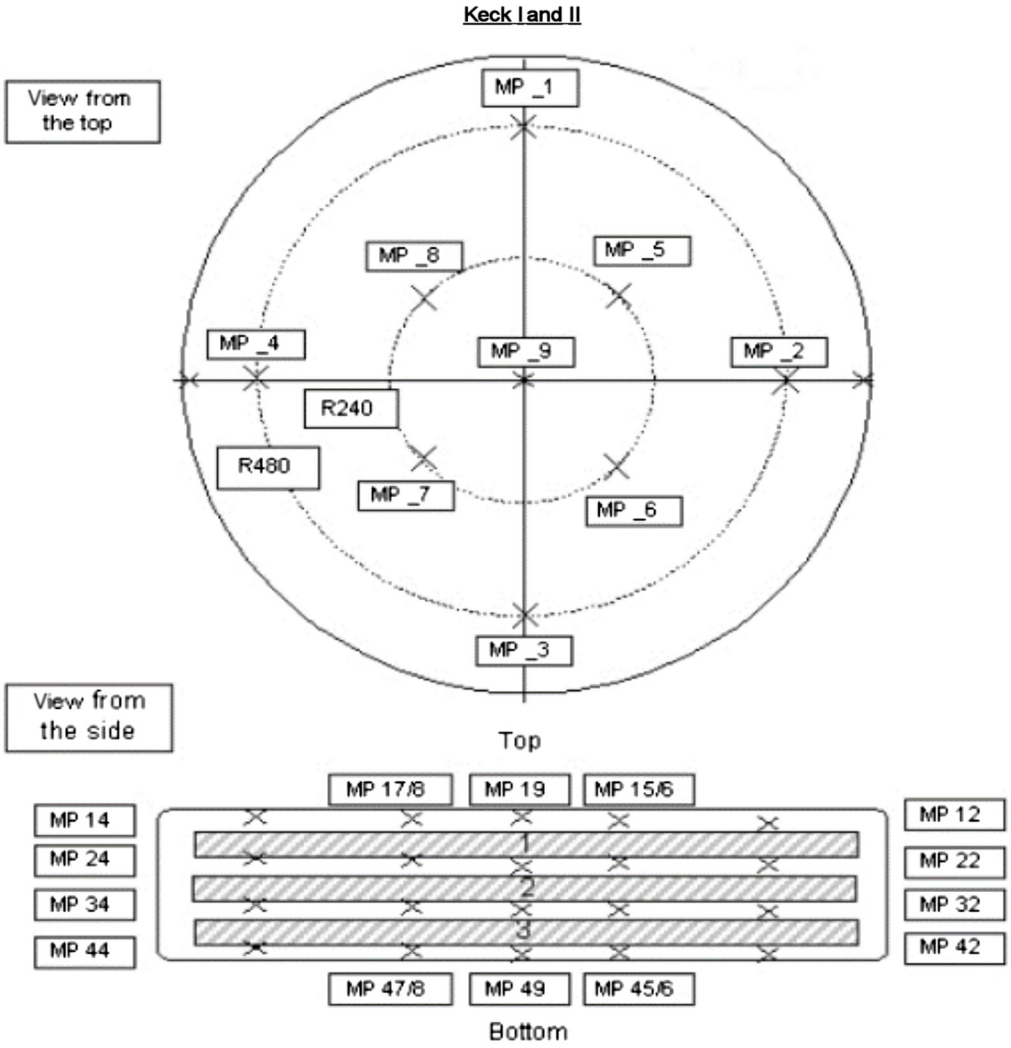

Fig. 1 Location plan for CTE measurement samples for the 2-m blanks of the Keck telescopes. One raw blank yielded three mirror blanks.[4] Explanation of numbering: MP *ik* means measurement point at position *k* according to top view in layer *i* according to side view. MP *ik*/*l* means point *k* or *l* in layer *i*.

The first is the homogeneity improvement achieved in the 1990s during the production of the ESO-VLT 8.2 m blanks. Special care was taken at that time to optimize homogeneity by investing in very large and precise tempering furnaces for the CTE determining ceramization process. At 700°C, the temperature variation across the almost 10-m wide furnace volume was kept close to 1 deg. Such precision in tempering capabilities allowed gaining additional experience in controlling the ceramization process with respect to the absolute CTE value as well as to its homogeneity. The two blanks delivered in 2003 and 2005 had been ceramized before the introduction of the new furnaces. The second step is the accuracy improvement of the dilatometer at Schott AG in 2005. The CTE measurement reproducibility of the advanced version was reduced by a factor 5 from 2.5 ppb/K down to 0.5 ppb/K (one standard deviation).

2.4 *Influence of the CTE Measurement Reproducibility on Homogeneity Results*

According to its definition as the difference between the highest and the lowest CTE measurement value, CTE homogeneity will always be larger than zero. Its determination method will always yield a result larger than the real homogeneity existent in the material blank. It renders a finite positive value even for perfect material blanks. The reason is that each of the single sample

Table 1 ZERODUR® 4-m blanks delivered between 2003 and 2019. Absolute CTE (0°C; 50°C) and CTE homogeneity values. *T*: 9°C ± 3°C: tailored to temperature interval 9°C ± 3°C.

Year	Dimensions (mm)	Number of samples #	CTE (0°C; 50°C) absolute value (ppb/K)		CTE (0°C; 50°C) homogeneity (ppb/K)	
			Specification	Achieved	Specification	Achieved[a]
2003	4100 × 171	18	±50	66	20	18 (14.6; 2.5)
2005	3610 × 370	12	±100	80	30	25 (23.5; 2.5)
2009	3700 × 163	36	±150	54	40	9 (8.5; 0.6)
2010	3400 × 180	12	±100	42	30	5 (4.7; 0.6)
2012	4250 × 350	16	±30	60	40	5 (4.6; 0.6)
2014	4250 × 350	16	±30	0	40	3 (2.0; 0.6)
2016	4060 × 103	16	±50	36	20	7 (6.7; 0.5)
2016	4000 × 100	12	±150	15	20	4 (3.6; 0.5)
2018 ELT M2	4250 × 101	20	±20 (*T*: 9°C ± 3°C)	–8	20	5 (4.5; 0.5)
2019 ELT M3	4000 × 101	20	±20 (*T*: 9°C ± 3°C)	27	20	4 (3.4; 0.5)

[a]In brackets, first number: homogeneity values with statistical bias caused by reproducibility removed, second number: reproducibility of measurement one standard deviation (see Sec. 2.4).

measurements is subject of the reproducibility statistics. The homogeneity result is the difference of the two samples with the extreme positions, the peak-to-valley values, which statistical variations will exaggerate in any case. For a set of 16 measurements as used for 4-m blanks, the mean measured CTE homogeneity for in reality perfect homogeneity will be 9 ppb/K with 2.5 ppb/K reproducibility and 1.8 ppb/K for 0.5 ppb/K reproducibility.

This relation can be demonstrated by creating statistical distributions using the Monte-Carlo method (see Fig. 2). For 16 CTE measurements points, 3600 data points were created each time using a random number generator for a normal distribution with the mean value CTE = 0 ppb/K. This simulates perfect homogeneity. The measurement reproducibility has been assumed to be 2.5 ppb/K or 0.5 ppb/K (one standard deviation). The normal distributions will

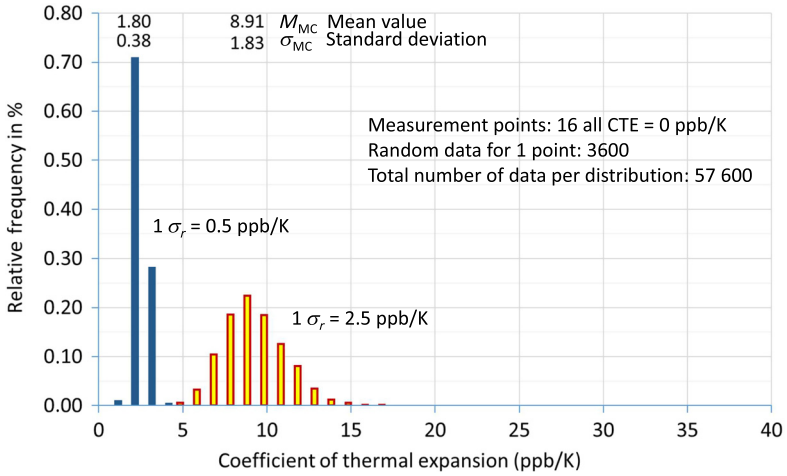

Fig. 2 CTE homogeneity measurement statistical distributions for a perfect (ΔCTE = 0 ppb/K) blank measured with CTE dilatometer of 2.5 ppb/K reproducibility (yellow) and with 0.5 ppb/K reproducibility (blue). Monte Carlo simulation based on 3600 random data per expansion measurement sample.

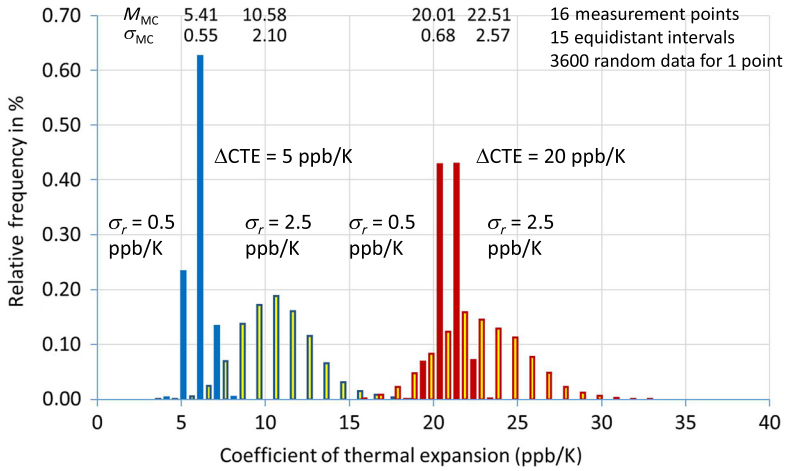

Fig. 3 CTE homogeneity measurement statistical distributions for two blanks with different "real" CTE variations (ΔCTE = 5 and 20 ppb/K) measured with CTE dilatometer of 2.5 ppb/K reproducibility and with 0.5 ppb/K reproducibility. Monte Carlo simulation based on 3600 random data per expansion measurement sample.

be symmetric since the absolute CTE of ZERODUR can be negative. The differences of the maximum and minimum of each of the 16-point data sets were sorted into the histograms shown in Fig. 2. The 2.5-ppb/K reproducibility measurement results in a homogeneity distribution with a mean value of almost 9 ppb/K for a perfect blank with 0 ppb/K in reality. The 0.5-ppb/K reproducibility distribution reduces the false homogeneity value down to 1.8 ppb/K.[10]

Monte-Carlo distributions for data sets including a "real" deviation from perfect homogeneity show that the deviation from "real" to "measured" results are strongest at and close to zero (see Fig. 3). The distributions were created as before but with the full "real" interval ΔCTE divided in equidistant subintervals. For ΔCTE = 5 ppb/K, the 2.5-ppb/K reproducibility leads to a mean value of 10.5 ppb/K. This is twice as large as "real." For 20 ppb/K, it is with 22.51 about 10% too high. For the 0.5-ppb/K reproducibility, overestimations are only about 10% (5.41 ppb/K) for 5 ppb/K real variation and 0.25% (20.05 ppb/K) for 20 ppb/K real variation. This is a substantial improvement in reducing bias inhomogeneity resulting from the measurement limitations.

Applying these findings to Table 1 and considering the systematic CTE homogeneity deviations outlined above, one can say that the CTE homogeneity has been improved by a factor more than 4 from about 20 ppb/K down to <5 ppb/K. The gain in homogeneity obtained on the occasion of the ESO-VLT 8.2-m production was preserved since then as the ongoing list shows.

Another example of the progress in CTE homogeneity is the results of measurements evaluated during the production of segmented 10-m telescopes. The two Keck telescopes were produced in the 1980s and early 1990s, and the Grantecan telescope in the early 2000s. Results for 89 2-m disks (Keck) and 42 2-m disks (Grantecan) allow comparisons between real measurements and simulations and the average CTE homogeneity of both projects.

Figure 4 shows the results for the 42 Grantecan disks. The simulation is based on 12 CTE measurement points with 2.5 ppb/K reproducibility and 4 ppb/K homogeneity for each disk. The match between both distributions is satisfactory. The distribution of the Grantecan data displays a larger skew, as it is expected for data sets with a small number of measurement points. A similar re-evaluation of the Keck I and II CTE data result in an average homogeneity of 8 ppm/K. Comparing both projects shows an improvement in homogeneity with a factor 2. In any case, the real homogeneity values are considerably better than the measurement results reflect and thus further below 20 ppb/K, which was the tolerance limit for both projects.

2.5 *CTE Homogeneity with Higher Spatial Resolution*

The CTE homogeneity measurement described above requires samples which are extracted from locations separated from each other by distances extending from one-third of a meter up to one

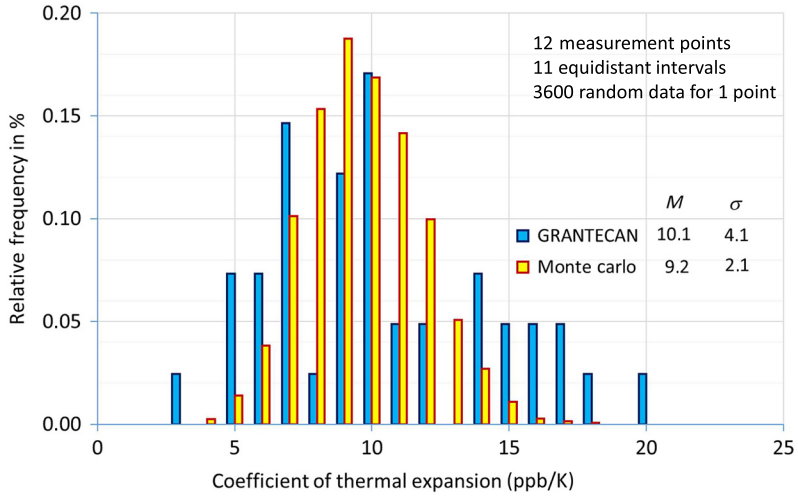

Fig. 4 CTE homogeneity of 41 ZERODUR blanks manufactured for the 10-m telescope Grantecan (blue). Measured data compared with Monte-Carlo simulation (yellow) based on "real" homogeneity of 4 ppb/K and 2.5 ppb/K reproducibility.

meter or even more in case of the 8.2-m blanks. In the early planning phase of the extremely large telescopes of the 30-m class, the question was raised if the outstanding homogeneity is given also on shorter scales both in radial and in axial directions. In order to answer this question, Schott cut disks from the middle of two 1.5-m diameter and 345-mm thick ZERODUR boules. 90 samples were taken from each disk. Along one diameter 28 samples allowed a spatial resolution of about 50 mm, along the perpendicular diameter 14 samples rendered 100-mm resolution. The 48 other samples covered the space in between the two main diameters (see Fig. 5).[5,11] The first disk (see Fig. 6 left) showed a homogeneity of 6.4 ppb/K. Within a 1.3-m diameter, the obtained values varied within 4 ppb/K without an observable trend. Toward one edge, the variation of about 4 ppb/K was significant beyond statistical noise. The second disk (see Fig. 6 right) showed a purely statistical pattern with the CTE variation of 3.8 ppb/K peak-to-valley. MC-simulation results with 1.8 ppb/K real CTE variation are compatible with this value. From both boules, also

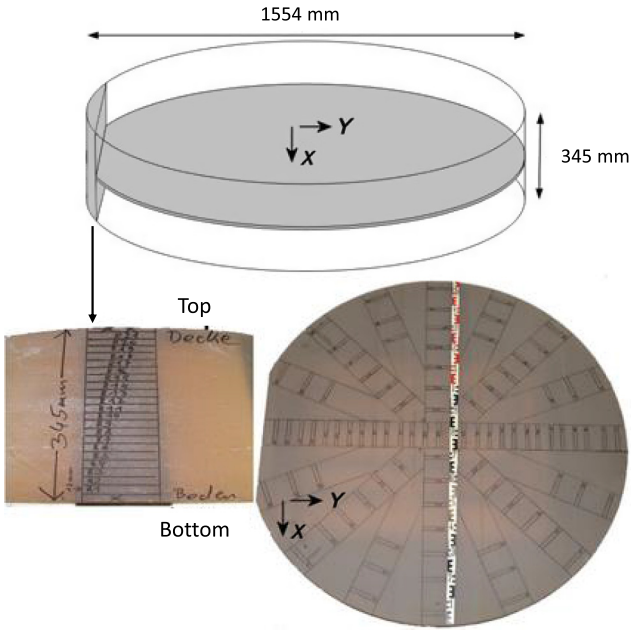

Fig. 5 CTE homogeneity of a 1.5-m ZERODUR boule sampling plan for horizontal and vertical distribution.[5]

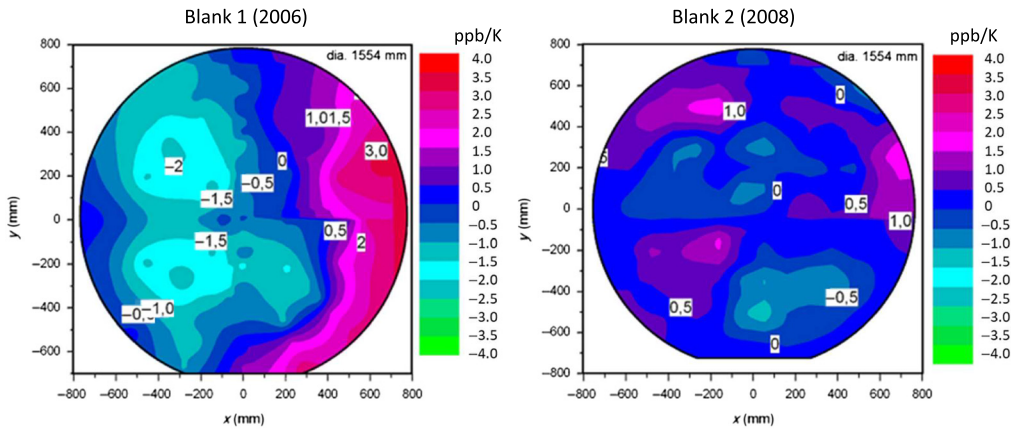

CTE (ppb/K)	Blank 1	Blank 2
Mean (0 °C; 50 °C)	42.4	39.9
Homogeneity (p-v)	6.4	3.8
Mean axial gradient 50 mm thickness	1.0	0.5

Fig. 6 CTE homogeneity with high spatial resolution for two 1.5-m ZERODUR blanks measured according to the sampling plan of Fig. 5.[5,11]

a vertical cut was taken. Twenty-one samples along the original 345-mm thickness render a 15-mm spatial resolution. The mean axial CTE variation within 50-mm thickness is 1 ppb/K for the first disk and 0.5 ppb/K for the second one. In 2019, a third disk measured with 93 measurement samples and 0.5 ppb/K reproducibility confirmed the long-term quality with an overall CTE homogeneity of 5.3 or 4.0 ppb/K with bias removed.[10]

ZERODUR structures used in microlithography are rectangular. Consequently, the cast blanks are designed to be also rectangular although the casting of round disks is more natural with all flow paths being equally long from the center. Therefore, there was some concern, if high homogeneity can be achieved especially in the corners of a rectangular blank. A measurement of a 1.2×1.2 m^2 square plate cast as a rectangular blank using 64 samples verified that its homogeneity is as excellent as that of round disks.[12] The CTE pattern shows no significant trend (see Fig. 7). The homogeneity result of 5 ppb/K reduces to 4 ppb/K if the 0.5 ppb/K reproducibility contribution is removed based on an MC simulation.

The highest possible spatial CTE resolution was achieved using a 100^3 mm^3 cube cut from a large square shaped ZERODUR production format in 2.2 m $\times$ 1.7 m $\times$ 0.3 m size[13] (see Fig. 8). A number of 100 samples taken in the pattern of a 10×10 matrix with a distance of 10 mm between two neighboring samples were measured using the dilatometer with improved accuracy (see part 1 of this paper). The peak-to-valley result of 1.3 ppb/K (see Fig. 9) was even better than 2.5 ppb/K, which is to be expected from the 0.5-ppb/K reproducibility. Possibly, the reproducibility conditions were especially good with this measurement, as 0.5 ppb/K is the more conservative long-term value.

2.6 *ZERODUR CTE Homogeneity Conclusion*

From the beginning of its use in large sizes, ZERODUR was a highly homogenous material. In the mid-1990s, further improvement was realized. However, the available measurement equipment was not capable to reflect this fully. Only with the dilatometers newly developed because of requirements for further reduced CTE homogeneity tolerances, it became possible to prove CTE variations to be in the lower single digit ppb/K range even for 4-m mirror blanks. The results compiled in Table 1 show that this quality level is maintained now for more than 10 years. High spatial resolution measurements confirm that the CTE homogeneity prevails along long (meter-sized) and short (centimeter) scales.

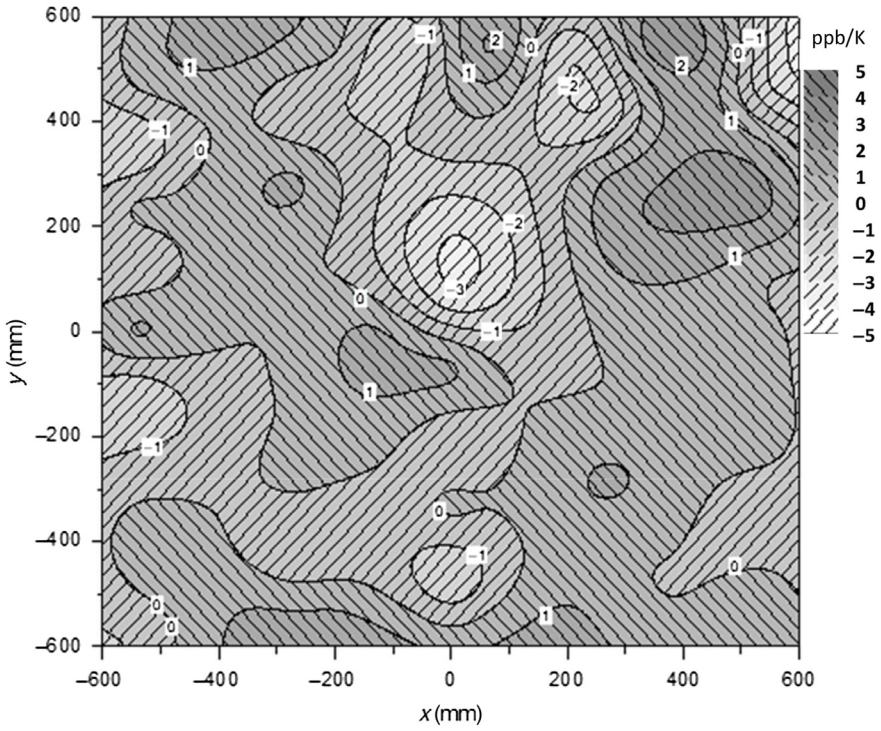

Fig. 7 Two-dimensional contour plot of CTE homogeneity value delta to the mean absolute value of 12.2 ppb/K of the 1.2 m × 1.2 m ZERODUR blank. The peak to valley homogeneity is 5 ppb/K.[12]

Fig. 8 ZERODUR cube 100 × 100 × 100 mm^3 cut in 100 samples.[13]

The CTE homogeneity of ZERODUR and the capability to prove it for given blanks have reached a point that demonstrates the suitability of this material for applications with extreme requirements even for very large sizes.

3 Material Homogeneity (Inclusions, Striae, and Stress Birefringence) and Reproducibility

Talking about the homogeneity of a material usually refers to its key property such as the refractive index of optical glass or the CTE of low expansion materials. However, there is a

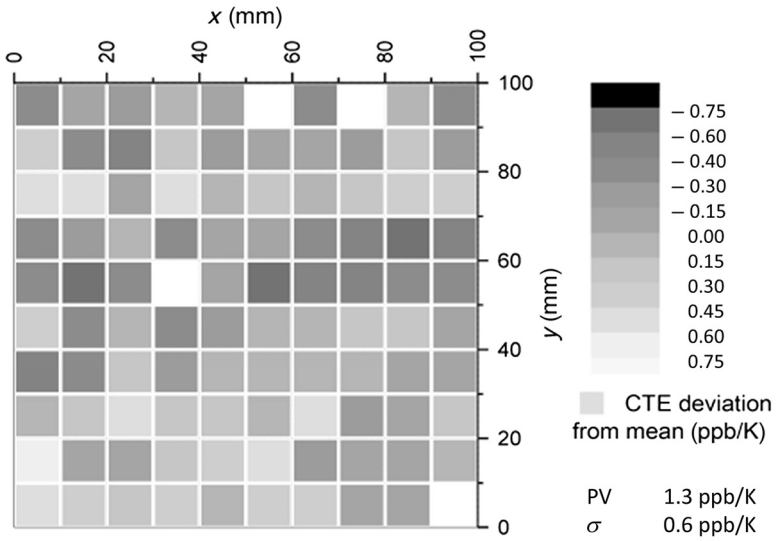

Fig. 9 CTE homogeneity of the $100 \times 100 \times 100$ mm^3 ZERODUR cube. The four white gaps represent broken samples.[13]

considerable set of other properties for which homogeneities are also prerequisites for the successful material application.

3.1 *Types of Material Homogeneity Deviations*

It starts with the simple question: is the same material present everywhere in the volume? There might be small partial volumes containing different materials: inclusions such as hard particles coming from incomplete melting or impure raw material. Bubbles might remain from imperfect refining, which is a part of the melting process. Each material has its own types of inclusions.

It continues with anisotropy, another form of inhomogeneity, the change of properties along different directions. Anisotropy can exist even in the ideal material itself; for example, along the different spatial axes in crystals. It might also result from preferred directions occurring in the production process. Examples are layers formed during physical vapor deposition or flow directions in glass melts resulting in striae. Inhomogeneous tempering will cause anisotropic stress fields, which are observable as birefringence.

Finally, the material itself might set a homogeneity limit. Detectable variations might arise with characteristic distances while traveling down the length scale in order-of-magnitude steps before reaching the atomic level. When applying a fictive microscope with ever-increasing magnification, the question is, in which typical length will separable components become visible? For ceramics, this will occur at about 1 μm, the typical size of powder grains; for ZERODUR, this will be at about 50 nm because of its nanocrystals.

The very small size of the crystals is another property of ZERODUR that sets it apart from ceramics. It is transparent even in the long-wavelength visible range. Part of its absorption in the green to violet range comes from Rayleigh scattering at the nanocrystals, which falls off toward longer wavelengths with the fourth power. For thicknesses up to about 500-mm internal quality, inspection can be done with visible light (see Fig. 10). For even thicker pieces, such as for example the boules made for the CHANDRA x-ray satellite with 1-m thickness, short-wave infrared cameras allow looking inside and even completely through them.[14] Due to the extreme optical homogeneity of ZERODUR, transmitted images are of such a high quality that one has to convince oneself, that the material is really in the light path.

All types of material inhomogeneity will impair the shaping and especially the polishing, possibly even the application of the material. Therefore, all vendors put special effort in their production processes for achieving best material homogeneity. Generally, the larger the pieces are, the higher is the challenge.

3.2 *Visual Inspections*

All ZERODUR casts are inspected with respect to their content of inclusions, striae, and stress birefringence.

Figure 10 shows the inclusion inspection of a 4-m ZERODUR blank with rear-side illumination. The vast majority of inclusions are bubbles. Other types are very rare. The inspection comprises search of the bubbles and determining their locations and sizes allowing optimization of the position of the finished blank in the raw cast blank. The so-called critical zone defines a volume lying some millimeters around the polished face's virtual position. Shifting the virtual position of the final blank within the raw blank allows achieving the best quality in the critical zone. This procedure reduces the risk of an open bubble in the face to be polished. The bubble content of ZERODUR is very low—the mirror blank for the ESO-VISTA telescope for example contained 31 bubbles in the size range between 0.1 and 2.7 mm in the total blank of 5.3 tons weight.[15,16] This together with the quality optimization in the critical zone makes an open bubble in the polished face an extremely rare event

Striae are localized slight changes in the material's composition. Strong striae are visible already in the inclusions inspection. Polarized light illumination enables detecting weaker striae. The shadow-graph method is the most sensitive method. The light of a point-like source will create shadows on a screen, when the material in the light path contains striae. It is capable to detect very faint striae with optical path length change down to 10 nm.

There are several quality grades available for the striae content. Strong striae are not admissible in any case. For most applications, standard striae quality is sufficient. Tests on ZERODUR blanks confirmed that weak striae have no effect on the local CTE.[17] Some applications of ZERODUR in transparency needed the best striae quality. Schott was able to deliver 2-m blanks with striae quality comparable to the best optical glass.

Stress birefringence is a material anisotropy resulting from inhomogeneous tempering. Since any heat treatment needs raising and lowering the temperature thermal gradients will occur within a material especially if it is a low thermal conducting one such as ZERODUR. The thermal gradients, which are present while crossing the transformation temperature range, result in a permanent mechanical bulk stress at room temperature. This stress is observable as birefringence. The stress in a ZERODUR blank is very low and varies only slightly over long distances across its volume. In circular blanks, it is central symmetrical and rises smoothly toward the edge. This is the reason why the measurement points lie close to the edge. Additionally, measurement conditions are easier here because one component of the stress tensor, the radial component, is zero. With the use of the de-Senarmont and Friedel method, birefringence can be measured very precisely down to one-tenth of a nanometer optical path difference.[18–21] All stress values in the volume are smaller than those measured close to the edges. An overall visual check

Fig. 10 Bubbles and inclusion visual inspection of a 4-m ZERODUR blank with radial coordinate system for inclusion mapping.

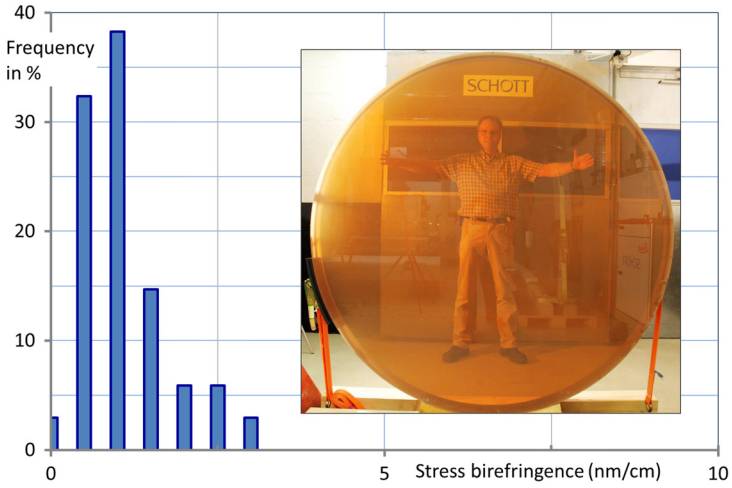

Fig. 11 Frequency of maximum stress birefringence values of 42 blanks with 2-m diameter manufactured for the 10-m Grantecan telescope. 3 nm/cm birefringence correspond to 0.1-MPa stress. Inset picture of a 2-m ZERODUR disk demonstrating its excellent internal quality.[18]

of a ZERODUR blank in front of a large polarizing light source serves for finding any irregularities in the stress field.

Figure 11 shows the stress birefringence results of the 42 ZERODUR blanks delivered for the Grantecan 10-m telescope. The highest value measured is 3 nm/cm optical path difference per thickness. The mean value is 1.3 nm/cm. With the stress optical coefficient of ZERODUR of 3.0×10^{-6} MPa^{-1}, these values convert to 0.1 MPa peak or 0.04 MPa mean bulk stress. These are very low values comparable to the best fine annealed optical glass. With 4-m mirror, blanks also stress birefringence values of 3 nm/cm have been achieved. Those of the four 8.2-m blanks for the ESO-VLT lie between 7 and 10 nm/cm.

3.3 *ZERODUR: a Highly Homogeneous Material*

ZERODUR is a homogeneous and isotropic material from 8 m down to 50 nm. It is free from rings, layers, seams, flaws, and pores (see Fig. 11 inset). Its volume is visibly inspectable. This helps greatly to prevent unexpected problems in downstream processes as might occur with intransparent materials. Figure 12 demonstrates its outstanding quality with three graphs of the same 200-mm ZERODUR disk. The first one shows it in lateral illumination free from inclusions, the second one is the image on the shadow-graph screen free from striae, and the third one is the refractive index homogeneity map based on the wave front image of a laser interferometer revealing optical homogeneity as good as that of the best optical glass.

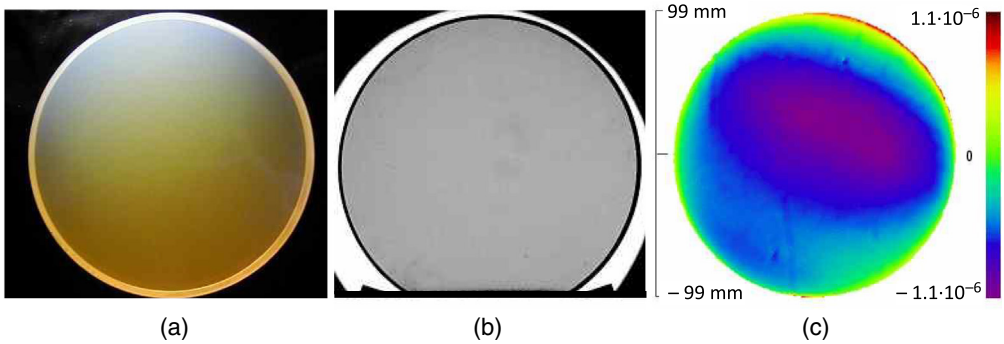

Fig. 12 Manifold homogeneity of a ZERODUR blank 200-mm diameter. (a) In lateral illumination: free from bubbles and inclusions; (b) screen image in the shadowgraph inspection setup: free from striae; and (c) refractive index homogeneity as evidence of extremely high homogeneity of all bulk material properties.

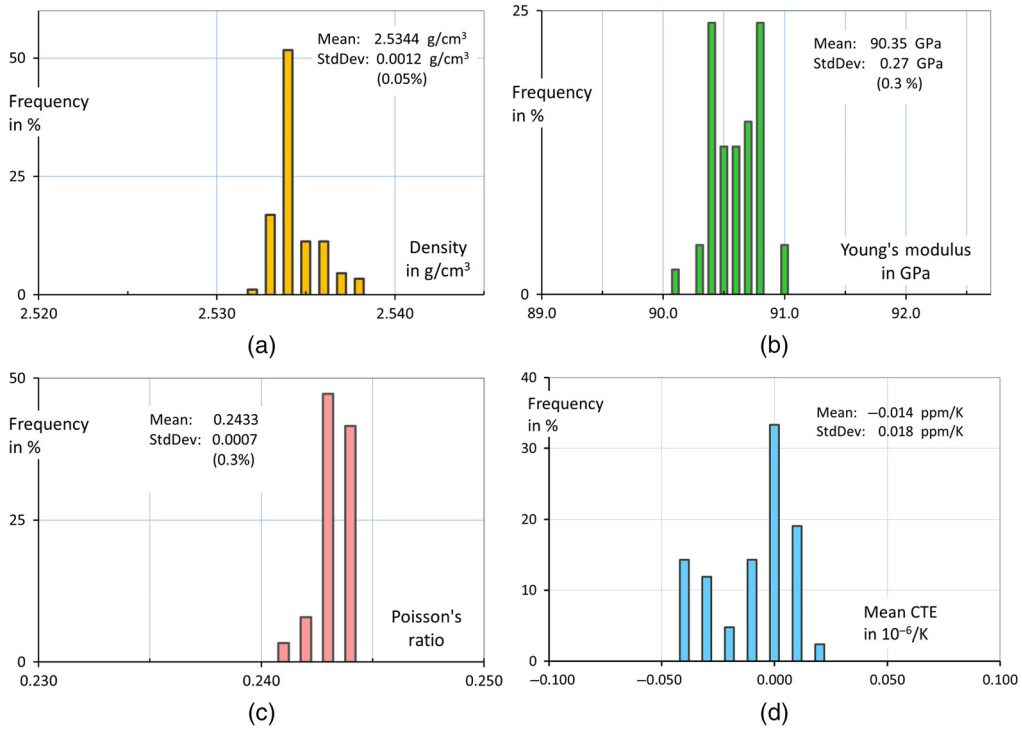

Fig. 13 Reproducibility of ZERODUR material properties based on data acquired from 2-m segments for the Keck and Grantecan telescopes. Data set size in brackets: (a) density (89); (b) Young's modulus (46); (c) CTE (42); [18] and (d) Poisson's ratio (89).

3.4 *ZERODUR: a Highly Reproducible Material*

Mirror or substrate design uses highly complex software in order to optimize their properties for the best application performance. Essential parameters for such calculations are typical material properties such as density, Young's modulus and Poisson's ratio. Even for individual pieces they are essential, but for large series of elements it is even more important, that the typical properties' data are reliable. The production process, its monitoring, and quality assurance procedures must guarantee sufficiently high reproducibility of the material properties. On the occasion of telescope projects, the high level of reproducibility for the mentioned properties has been demonstrated[18] (see Fig. 13). It shows histograms for the properties' density, Young's modulus, Poisson's ratio, and absolute CTE with data sets of sizes from 42 to 89 obtained from the Keck and Grantecan 2-m segments production. The observed variations lie fairly below 1% and come largely from the limited measurement accuracies. This also holds for the absolute CTE values, which were measured with the inductive coil dilatometer with an absolute CTE uncertainty of ± 10 ppb/K. This means that the already very narrow distributions will be even narrower in reality. The excellent reproducibility proves the outstanding mastering of the production process of ZERODUR.

4 Mechanical Strength

4.1 *Subsurface Microcracks Determine Practical Strength*

Considering the strength of their atomic bonds glass and glass ceramics should be very strong with theoretical breakage stress values fairly exceeding 10 GPa (Giga-Pascal). However, their practical strength lies several orders of magnitude lower. The reason is their high sensitivity against surface flaws. Environmental wear or technical grinding processes introduce subsurface microcracks [also referred to as subsurface damage (SSD)]. The cleavages of microcracks in glassy materials reduce to nanometer widths at their tips. They extend considerably deeper than

a roughness stylus with its tip rounded commonly to a micrometer radius can measure. Such microcracks will grow if surface tensile stress loads surpass a minimum value. For low-stress loads, crack growth is very slow if happening at all. Glass items under such loads can survive for many years.

The preparation of a ZERODUR mirror substrate or structure implies creating surfaces with different functions. For the shaping of the faces, one uses grinding processes. Fast rotating tools with bound hard grains—usually diamond grains—introduce microcracks into a surface layer and then remove the material by chipping it off. Consequently, subsurface microcracks will remain in all finished surfaces. Depending on the grain size used for the final process step, they will differ in their depths and number per area. The optimization criteria for the generation of the lateral faces are usually economics leading to the use of coarse grain tools for efficient grinding. If not otherwise required they will remain in this condition. The reflecting mirror surface will be prepared using grinding steps with ever-finer grains prior to polishing in order to reduce stray light. As a side effect, polished surfaces have much shorter microcracks than coarse-ground surfaces. The deepest microcrack present in the surface determines its mechanical strength. This leads to the interesting observation that the strength variation between coarse ground and polished surface conditions for a given material might be greater than the variation among very different glassy materials ground with grains of the same size.

4.2 *Three-Parameter Weibull Distribution Characterizing Statistical and Deterministic Breakage Behavior*

In technical ground surfaces, there are a huge number of microcracks. There can be 10,000 and more per cm^2. The deepest one of all these many microcracks in a homogeneously tensile stress loaded area determines the breakage stress. Each stressed surface has its own deepest microcrack. Considering a sample of such stressed surfaces in order to predict their behavior under given loads means to deal with the statistics of these largest microcracks. The extreme value statistics used in brittle materials breakage analysis for the failure probability $F(\sigma)$ depending on the surface tensile stress σ usually given in mega-pascal (MPa) is the Weibull distribution:[22]

$$F(\sigma) = 1 - e^{-\left(\frac{\sigma-\sigma_T}{\eta}\right)^{\beta}}, \tag{1}$$

σ_T is the location parameter—threshold breakage stress, η is the scale parameter, and β is the shape parameter.

The three-parameter Weibull distribution renders satisfactory fits to the data as demonstrated in a set of investigation results.[23] Its location parameter σ_T is equivalent to a stress threshold. Above this threshold failure probability rises with increasing stress, below it the failure probability is zero,[24] just as it is expected for brittle materials with surfaces with a maximum microcrack depth. The general crack growth law for glass and glass ceramics states that the growth velocity depends not only on the tensile stress but also on the initial crack length. For each crack length, there is a minimum stress, which must be surpassed to start crack growth eventually leading to breakage. This fact is also the basis of the proof test, a method employed for very safety critical items from brittle materials. Prior to their use for example as windows used in manned space flight, they are subjected to test loads surpassing the final application load. If they pass the test, it means that the maximum microcracks in the different parts of their surfaces are all smaller than the admissible overall maximum microcrack.

Just as with the proof test, one can determine a threshold stress for each type of SSDs introduced by a well-defined grinding process. The zero breakage probability below the threshold stress increases the prediction reliability for stress load applications tremendously.[25]

4.3 *Breakage Stress Measurement Method*

The common method to measure the dependence of the breakage failure probability on tensile stress for a given surface condition is breaking a sample of specimens using a double ring test setup according to the European standard EN 1288 part 5 (see Fig. 14). This setup provides a very homogeneous and isotropic stress field inside the loaded test area. Outside of this area, the

(a) (b)

Fig. 14 (a) Taking of 100 mm × 100 mm × 6 mm tiles for breakage stress measurement from a ground ZERODUR® plate lying on a ZERODUR boule as support. (b) Laboratory ring-on-ring setup, the specimens will lie on the support ring while stress is being introduced with the upper five times smaller load ring.[25]

stress drops sharply reducing breakages with undefined conditions strongly that have to be discarded from evaluation. The specimens—disks or plates—are ground with the tool and process conditions to be investigated. Any residual microcracks from preceding process steps have to be eliminated carefully by grinding off a layer with a minimum thickness. The stress is raised linearly usually by 2 MPa/s until the specimen breaks. The stresses at breakage are recorded for a sample of specimens. In order to verify the three-parameter Weibull statistical distribution as the valid representation of the data with sufficient statistical significance one needs a high number of specimens of about 100 to 170 per sample at minimum. If its validity is already proven, only 30 to 60 specimens are sufficient to determine the three distribution parameters.

4.4 *Breakage Stress Measurement Results*

Figure 15 shows breakage stress distributions for different surface conditions of ZERODUR: diamond grain ground (dark blue, purple), etched (light blue, red), and polished (green). The Weibull distribution fits well to the data of the D151 (coarse grain) and D25 ground (very fine grain) surfaces and the optical polished surface. The investigated etched surfaces have more than one breakage mechanism. Therefore, the Weibull distribution does not fit. Typically, for surfaces with smaller SSDs, the threshold shifts to higher breakage stresses and the distribution becomes wider.

4.5 *Fatigue with Long-Term Loads*

With the widely used stress increase rate of 2 MPa/s for breakage tests, breakage occurs within seconds or minutes. Consequently, the statistical stress distribution obtained holds only for very short-term loads. For long lasting loads, a fatigue effect becomes important, the growth of the microcracks. Their growth speed depends not only on their depths and the applied stress but also on the environmental conditions especially on humidity. The presence of water enhances microcrack growth. In order to characterize fatigue, only one parameter is needed: the stress corrosion coefficient, abbreviated with the letter n.[26,27] The same ring-on-ring setup as used for the breakage measurement serves for determining the stress corrosion coefficient. Several samples are measured with largely differing stress increase rates. Since the crack growth velocity depends

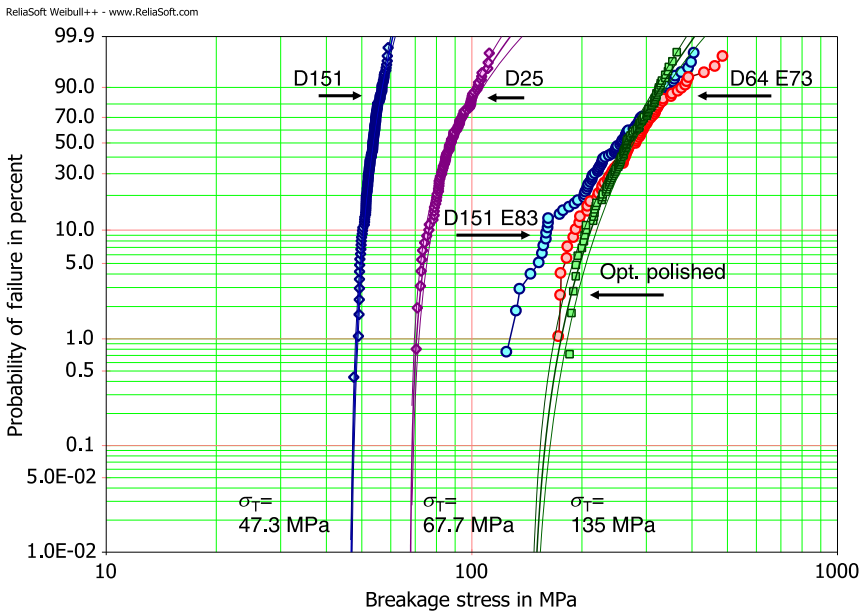

Fig. 15 Weibull plot of five ZERODUR samples, three of them with three-parameter Weibull distributions fitted and 90% confidence bounds. Two samples are ground, one with coarse grain (D151, dark blue) and one with very fine grain (D25, purple). Two samples have been ground and subsequently etched (D151 E83, light blue and D64 E73, red, coarse, and finer grain surfaces with 83 and 73 μm etched off, respectively), one sample consists of optically polished specimens (green). For the fitted samples the threshold stresses are given. The etched surfaces distributions also tend to a minimum breakage stress value. The Weibull plot uses a double logarithmic y-axis rendering a curve for the three-parameter Weibull distribution and a straight line for its two-parameter version.

on n exponentially, different values lead to huge differences in prediction calculations. Loading brittle materials in vacuum reduces fatigue tremendously compared with normal humidity air.

4.6 *Minimum Lifetime for Constant Loads*

Applying the well-established crack growth law for brittle materials on the threshold breakage stress allows deriving a minimum lifetime calculation model including the fatigue effect. In this model fatigue shifts the breakage stress threshold from its short-term value to lower values according to the applied stress and its duration (see Fig. 16). Note the strongly non-linear shift between the values obtained with the laboratory tests with time to breakage of seconds to the long-term values. Equations (2) and (3) allow predicting the empirical minimum lifetime $t_{B,c}$ for a given constant stress value $\sigma_{B,c}$, or calculating the allowable maximum constant stress $\sigma_{B,c}$ for a required minimum lifetime $t_{B,c}$:[24,25]

$$t_{B,c} = \frac{\sigma_T^{n+1}}{\sigma_{B,c}^{n}} \frac{1}{(n+1)\dot{\sigma}_r}, \tag{2}$$

$$\sigma_{B,c} = \left[\frac{\sigma_T^{n+1}}{t_{B,c}(n+1)\dot{\sigma}_r}\right]^{\frac{1}{n}}, \tag{3}$$

where $t_{B,c}$ is the minimum lifetime, σ_T is the breakage stress threshold measured with constant stress increase, $\sigma_{B,c}$ is the constant stress load, the design strength, $\dot{\sigma}_r$ is the constant stress increase rate during measurement (Schott standard value 2 MPa/s), and n is the stress corrosion coefficient representing the fatigue effect (ZERODUR normal humidity $n = 31$, dry $n = 50$, and vacuum $n = 79$).

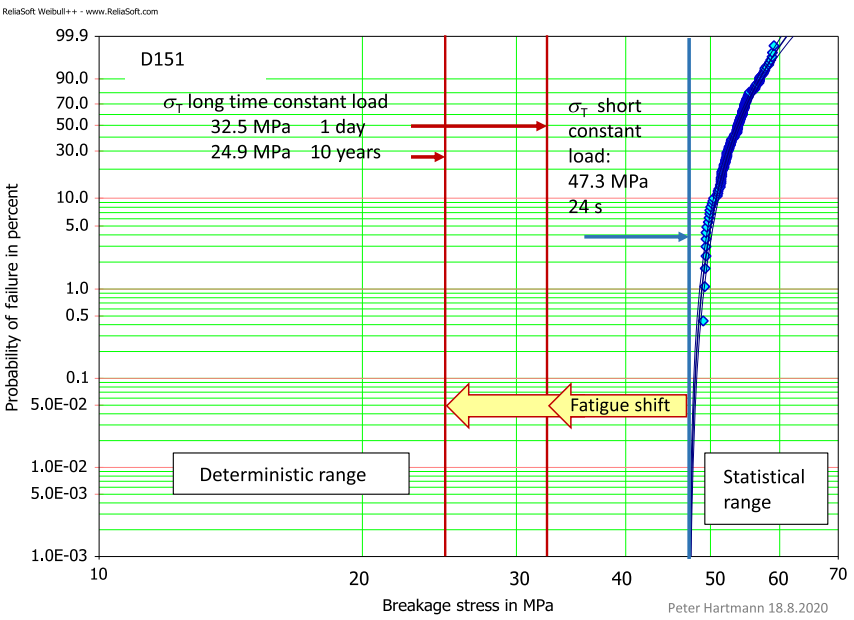

Fig. 16 ZERODUR D151 sample with threshold stress at 47.3 MPa valid for short-time loads (24 s). The threshold stress σ_T divides stress in a deterministic and a statistical range. Due to stress corrosion the admissible threshold stress for a 1-day constant load shifts down to 32.5 MPa and for 10 years to 24.9 MPa (for normal humidity environment).[23]

4.7 *Influence of Surface Quality on Lifetime or Allowable Stress*

It is possible to increase the strength of an item from brittle material either by polishing or by etching. In both cases, the underlying mechanism is the removal of the subsurface microcracks.

In any case, it is essential to avoid reintroducing microcracks. This can occur during handling, transport, and installing of the glass ceramic item. It might reduce the improved strength considerably. The sensitivity of etched and polished surfaces is different. Etching introduces a surface microtopology. Tiny pits overlap and form ridges and tips. Touching surfaces with such textures might lead to chipping off from tips and ridges, thus introducing microcracks again. This makes etched surfaces sensitive against touching. Such microdamages do not lead to a total loss of strength increase, but they prevent exploiting the full potential of strength increase by etching. Polished surfaces remain being flat even on the micron scale. Therefore, they have less contact surface for producing microdamages and are somewhat less sensitive against touching.

For etched surfaces, the Weibull distribution is not adequate anymore. Its presupposition, a sample with statistically distributed elements of comparable weakness with one of them being the weakest, is not given anymore. At least, it is not observable on the present experimental data basis. This is because strength improving etching according to specification removes all microcracks. There are no cracks with sharp tips left over anymore. The origin of breakage of fully etched undamaged surfaces is not explored. Hence, also the statistical distribution of such breakages is unknown. Together with the additional occurrence of microdamages this results in mixed breakage statistics. Fitting of any Weibull distributions fails. Polished surfaces still follow the three-parameter Weibull distribution indicating that breakage still starts from sharp tips but of much shorter microcracks. Even if simple statistical description for etched surfaces fails, this does not mean that microcrack depth is not limited. Breakage stress thresholds still exist. They can be estimated from the breakage stress samples based on the lowest data points.

Figure 17 displays minimum lifetime curves for ZERODUR with differently prepared surfaces. The four curves on the left are valid for surfaces ground with bonded diamond grain tools of different grain sizes. The curve at the extreme left gives the lifetime for D151 ground surfaces. With a maximum grain size of 150 μm, it is a comparatively coarse grain frequently used for shaping of the lateral mirror face that does not require special strength. Up to 23 MPa constant load, the lifetime of items with such surfaces exceeds 50 years. The other three curves show the lifetime of samples with surfaces prepared with finer grain sizes of 46, 35, and 25 μm (left to

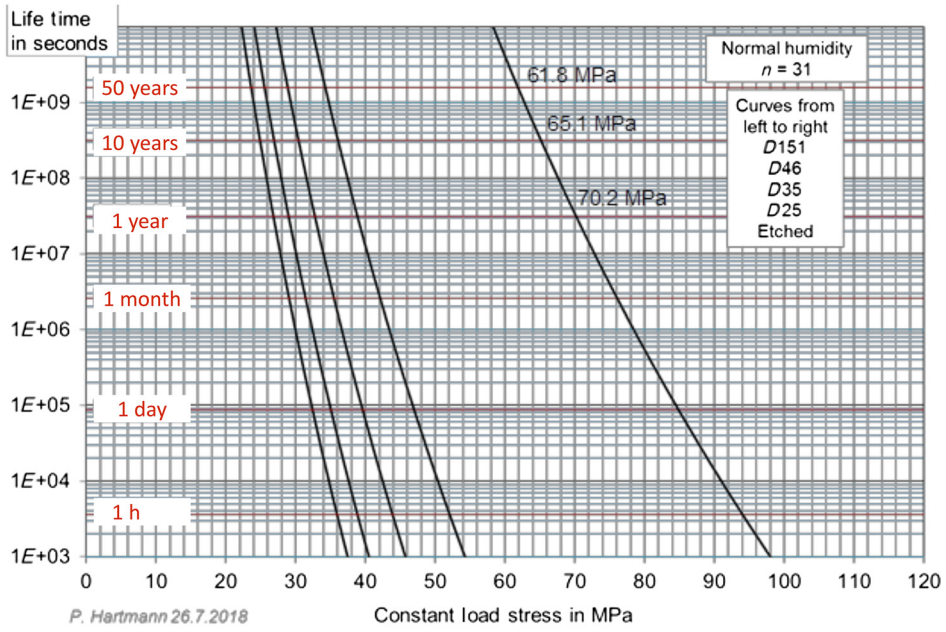

Fig. 17 Lifetime of ZERODUR items prepared with four different grinding tools, D151, D46, D35, D25, and ground and then etched in normal humidity environment ($n = 31$). For D64 ground surfaces, the D151 curve can be used because the threshold stress values are almost identical. The short-term threshold stresses for the D151 and D25 ground surfaces used for the calculations are given in Fig. 15. The short-term minimum breakage stress for the etched surface curve is 120 MPa. This holds for a surface with a layer etched off thicker than the maximum crack depth introduced by the preceding grinding process. For more information, refer to Ref. 25.

right) typically used for surfaces with enhanced strength requirements. A considerable increase in strength asks for etched surfaces. The curve on the very right side is valid for surfaces with a layer etched off, which is about as thick as the maximum size of the grains used to grind the surface before. Such surfaces can be loaded constantly for 50 years with 60 MPa. All predictions require that no additional surface flaws occur during the application period.

5 Melting, Casting, and Ceramization

This section gives only a very short overview of the production process of ZERODUR. For a detailed presentation, refer to the book of H. Bach.[1] In its first step, the production of ZERODUR is similar to that of optical glass. A mixture of very pure raw materials is filled into a large very hot container, the melting tank. When all raw materials are molten, any bubbles created by chemical reactions are removed in the refinement stage. Casting of blanks begins when the melt reached the required homogeneity. For large blanks, casting time must be kept short in order to keep all process conditions constant. Only discontinuous melting tanks are suited to fulfill this requirement. Ten tons or in the case of 8-m blanks 45 tons have to be cast into the moulds within a few hours with all temperatures and flow rates under precise control.

Directly after casting or if it is needed after a forming stage such as spinning to achieve a concave surface the cast will be cooled down as fast as possible (see Fig. 18). This is done to avoid any crystallization in the volume. It is one of the preconditions for the material that the temperature ranges for crystal nuclei formation (N) and for crystal growth (C) are separated. While cooling down, the melt crosses the crystal growth ranges first. However, since no nuclei exist in this stage, no crystals will grow. Later when crossing the nuclei formation range, any emerging nuclei will not grow to a crystal because in this range the growth rate is very small or zero. The fast cooling stops at the transformation temperature Tg, where the material begins to become rigid. Now the blanks in their moulds are put inside furnaces for slowing down the annealing rate because temperature gradients have to be reduced for keeping the internal stress

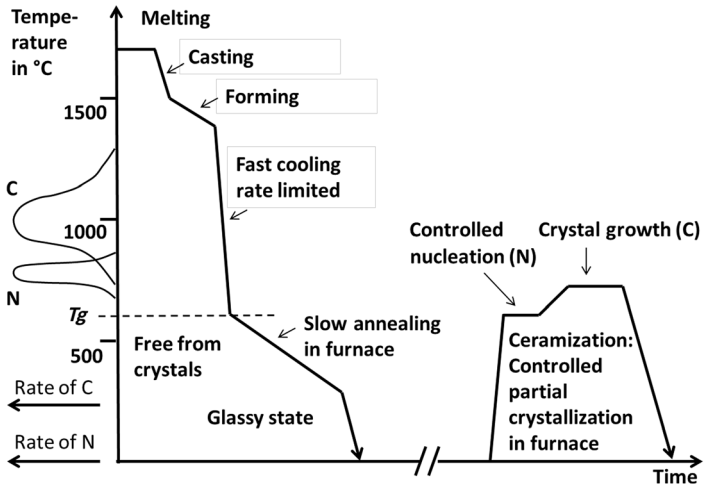

Fig. 18 Production of ZERODUR temperature versus time diagram. The first stage results in glassy ZERODUR, which has to be ceramized in the second stage called ceramization in order to acquire the close to zero expansion. Left from the *y* axis, the temperature range for nuclei formation and for crystal growth is indicated. *Tg*, transformation temperature.

low. About 150°C to 200°C below the transformation temperature cooling can speed up again but it is still limited to avoid breakage due to temporal stress caused by internal thermal gradients.

After reaching room temperature, the still glassy blanks with a CTE close to that of borosilicate glasses will be ground removing surface crystals and polished for the first quality inspection. The following ceramization process comprises two major steps, nuclei formation and crystal growth. Depending on the geometry of the blanks and the required expansion tolerance temperature–time programs have to be adjusted assuring the right number of crystals per volume and their size. The cooling rate is limited for achieving low permanent stress in the blank. The total production process from melting to ceramized blanks can last from three month up to 1 year. The main reason is the tempering time in the ceramization process. The larger and especially the thicker the blanks are, the slower any temperature change rate must be. Otherwise, temperature gradients occurring rapidly in low thermal conducting materials such as glass and glass-ceramics would impair the material homogeneity one of the key properties for application. This does not mean that any delivery will last that long. Schott casts a set of standard sized blanks regularly. For items up to 2 m, delivery times are much shorter. For larger items, it is recommended to contact Schott as early as possible.

The overall production capacity depends only on the number of existing melting tanks, their melting cycle time and the number of tempering furnaces (see Fig. 19). Since the turn of the millennia, the capacity for ZERODUR productions increased considerably due to the high demand from astronomical applications as well as for industrial applications. In 2019, Schott conducted a major program to expand their production capacity in response to the continuously growing demand from industrial application such as integrated circuits and flat panel display lithography, aviation and precision metrology, as well as for ground-based and space-born

(a) (b) (c)

Fig. 19 (a) Casting of ZERODUR; (b) tempering furnaces for cooling down melts and for ceramization; and (c) ZERODUR boule after ceramization.

telescope optics. The installed capacity easily covers any future industrial and science demands for the low thermal expansion glass ceramic ZERODUR.[28]

6 Shaping and Polishing: Lightweight Mirrors and Structures Grinding and Metrology

6.1 *From Simple to Sophisticated Shapes*

Originally, ZERODUR was developed and used for telescope mirrors for astronomical observatories. The mirrors were bulky and thick items with tolerances of several millimeters in their diameters. Only the mirror faces were highly precise as result of long-lasting and painstaking polishing processes.[2]

Applications outside astronomy emerged soon after the production of the first ZERODUR mirrors. Its combination of very low thermal expansion and very low Helium permeability made it a perfect substrate for ring laser gyroscopes. They improved position stability of airplanes tremendously. In the early 1990s, first precision mechanics structures were made from ZERODUR serving as supports and frames in microlithography. At that time, glass experts did not expect that complex and delicate components with features specified with tolerances in the 0.01-mm range could be made from a glassy and thus brittle material. However, the use of CNC-controlled grinding machines from metalworking with bonded diamond grain tools and adjusted work processes led to astonishing complex high-precision structures. Grown in size and complexity such structures are key components in present and future microlithography. The Dutch company Philips, whose Microlithography Department later became the company ASML, pioneered this work in Europe.

6.2 *From Lightweighted to Extremely Lightweighted Blanks*

Possibly inspired by this progress, the lightweighting methods for astronomical mirrors changed from drilled out holes to filigree rib structures on the backside. Prominent early examples are the 1-m secondary mirrors of the two Gemini 8-m telescopes (see Fig. 20).

In this case, Schott ground the backside rib structures to 8-mm-thickness and the company Carl Zeiss reduced it further to 4 mm by extensive etching.[29,30] The production of the 1.5-m primary mirror for the solar telescope GREGOR in 2010 marked the summit of complex lightweighting technology based on 8-mm rib thickness and allowing to reach weight reduction up to about 70%[31,32] (see Fig. 21).

At the same time, first technology demonstrators showed the possibility of producing highly lightweighted mirror substrates with weight reduction close to 90% only from CNC grinding with rib thickness down to 2 mm and almost 200-mm rib height. In 2011, Schott presented a 700-mm full featured lightweight mirror demonstrator with such rib dimensions. The faceplate backside followed the front face curvature. The backside of the structure was ground with a trefoil geometry as an example for the wide range of possibilities. The weight reduction amounted to 88%.[33]

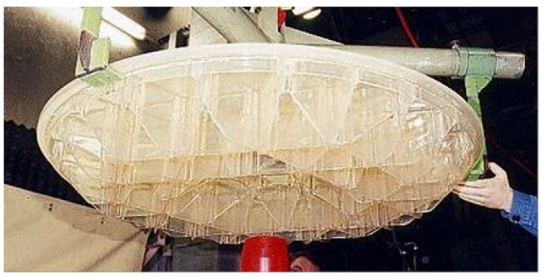

Fig. 20 GEMINI telescope 1-m secondary mirror with 4-mm rib thickness 45 kg 85% weight reduction.

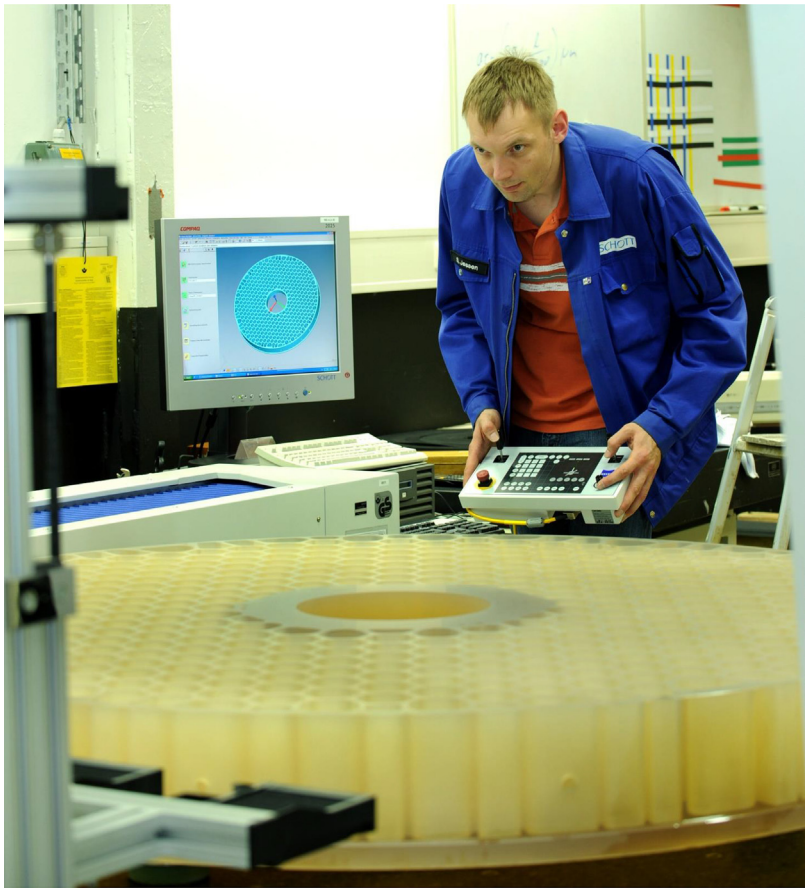

Fig. 21 Solar telescope GREGOR 1.5-m diameter × 161-mm-thick primary mirror, 420 pockets 8-mm rib thickness, and 65% weight reduction.

In the same paper, the company Brashear USA demonstrated that the so-called print-through or quilting effect can be avoided with the then available precision polishing technologies Magneto-Rheological finishing and computer controlled optical surfacing. This effect had caused unacceptably large local deformation and so prevented further reduction of the face sheet thickness and mirror weight. With new CNC grinding machines providing higher precision and flexibility in processing, tool changing, and process control, Schott was able to present a 1.2-m lightweighted mirror blank weighing only 45 kg at reasonable costs[34] (see Fig. 22). This mirror blank has been polished and tested as finished mirror for surface figure errors in thermal soak tests by NASA at the Marshall Space Flight Center in Alabama proving the technical readiness level TRL 6 for such lightweighted structures.[35,36] Comparing experimental data with finite-element simulation results confirm the very high CTE homogeneity of ZERODUR.

Further studies on dimensional upscaling up to 4-m diameter revealed the possibility of such large lightweight mirrors and provided guidelines for cost optimization.[37–40] A 4-m extremely lightweight ZERODUR mirror is a key component in the baseline concept of NASA's habitable zone exoplanet observatory HabEx.[41]

6.3 *Suitability of ZERODUR Extremely Lightweight Mirrors for Space Missions*

A common method to value the suitability of a material for a given application is to define figures of merit allowing ranking them. In valuing materials for lightweight space borne mirrors, one possibility is to use a diagram with the specific stiffness plotted against the thermal transient resilience (see Fig. 23). With marking the earlier published literature data point for ZERODUR together with the new point achieved with narrower CTE tolerances, the improvement reveals to be outstanding.[42,44,45]

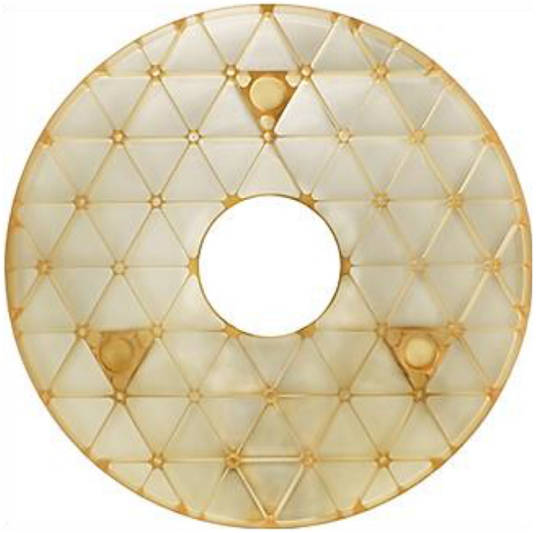

Fig. 22 1.2-m diameter × 125-mm thickness ZERODUR® lightweight mirror blank with 2-mm ribs, 44 kg at 84% weight reduction and lowest eigenfrequency of 209 Hz. Further design improvement allows reduction to 41 kg.

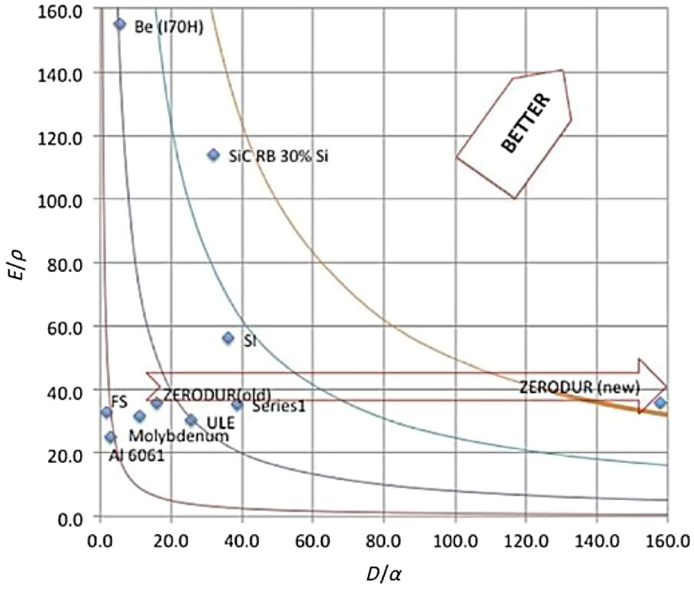

Fig. 23 Specific stiffness E/ρ plotted against thermal transient resilience D/α. E, Young's modulus; ρ, density, D, thermal diffusivity $= k/\rho c_p$ k-thermal conductivity; and c_p, specific heat. Materials: beryllium (Be), silicon (Si), silicon carbide (SiC), fused silica (FS), titanium-doped fused silica (ULE), aluminum (Al), molybdenum, and ZERODUR®.[42,43]

6.4 *Large Blanks with Sophisticated Geometrical Features*

Not only lightweight structures from ZERODUR profited from the progress in CNC machinery. The precisely controlled grinding processes allow solid large blanks with sophisticated geometrical features. The primary mirror of the DKIST solar telescope with its off-axis aspherical face is an outstanding example.[7] It was delivered in 2014 with a maximum shape deviation of the mirror surface of 160 μm. The recent investments in grinding machinery reduced the possible maximum shape deviation down to 30 μm with SSDs <15-μm deep.

An example for a recently produced 4-m mirror with special geometrical features is the ESO ELT 4.25-m secondary mirror with its extreme convex curvature (see Fig. 24).[40]

Fig. 24 ESO ELT ZERODUR® secondary mirror blank with 4.25-m diameter, 100-mm thickness, and extreme convex curvature as delivered from Schott in January 2019.

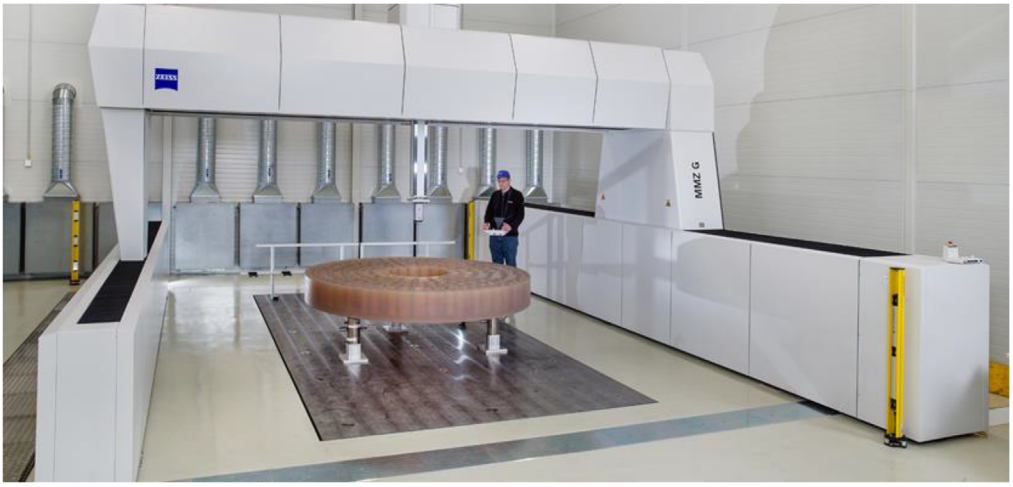

Fig. 25 Schott's new 5-m coordinate measuring machine with ZERODUR® lightweight mirror blank. Maximum measurable dimensions are 5 m × 6 m × 2 m. Temperature stability: better than 0.3 K per day. Maximum deviation found during calibration 2 μm at 2.5 m radius.

Progress in machining requires measurement equipment with higher accuracy. A new coordinate measuring machine at Schott accredited by the German National Bureau of Standards (DAkkS) provides versatile measuring capabilities in a volume of 5 m × 6 m × 2 m (see Fig. 25).[40] Its micrometer precision means a factor 10 improvement with respect to the formerly used laser tracker.

The very high gain in shaping and in inspection precision for mirror blanks with diameter up to 4.25 m helps reducing the preparation processes for polishing considerably. This saves not only time but also money since grinding is much more efficient than other preparatory shaping processes as for example lapping with loose grains.

7 Outlook

In microchip and in flat screen development, the ongoing trend points into the direction of higher feature densities of transistors or pixels on chips or panels. During the production, the required precision needs suppressing temperature influences to ever-smaller amounts. Only the combined use of all available methods, active—air conditioning—and passive—use of thermal insensitive materials, allows to achieve the required dimensional stability. The pressure for improving

stabilization methods continues on a high level. Fortunately, ZERODUR still had and has reserves in expansion reduction, which can be exploited for future tighter requirements. A great deal of this progress came from the close communication of astronomers with the material experts. Astronomers are well known for never being content with the achieved state of the art. Their continuous challenging of the materials experts has led to substantial improvement in their observatories and instruments resulting in high benefits also for other technical applications. New astronomical telescope projects will pose new challenges. Therefore, this review will not mark the end of the ZERODUR development but only an intermediate step. For continuing this success story, it is highly recommended to maintain the close communication between the material experts and the users also in the future.

8 Conclusion

Even though ZERODUR is a young material with 50+ years of existence, it is sometimes regarded as a classical material with all properties well known, settled, and fixed. Its history, however, shows that there was and is a continuing development in its properties and the related metrology as well as their characterization for various applications. This holds especially for the decades between 2000 and 2020. A broad set of improvements enabled new and wider applications supporting great progress in subsequent technologies.

These improvements are [the brackets refer to the part of this paper/the section/and the main references] as follows.

- The CTE guaranteed in narrower tolerance limits close to zero [1/3.2/23].
- The further reduction of thermal expansion by adapting the material to the special thermal profile prevailing in the specific application. This can amount to a factor of up to 10 with respect to the best CTE tolerance material [1/3.4/23, 27].
- The extremely high CTE homogeneity throughout the total volume of even 4-m diameter mirror blanks lies in the lower single digit parts per billion per Kelvin range. The high homogeneity is proven from long ranges with distances of 1 m down to short ranges with distances of 1 cm [2/2.3–2.5/9].
- The CTE measurement uncertainty could be restricted further down to ± 3 ppb/K absolute with 0.5 ppb/K reproducibility (one standard deviation) [1/4.3/43].
- The CTE is also low in the cryo temperature range and it is possible to adapt CTE close to zero from room temperature down to 100 K [1/3.6/35].
- Even the largest blanks up to 4 m in diameter are available with outstanding internal material homogeneity, which means very low content of bubbles and inclusions, permanent bulk stress, and striae [2/3/15].
- A meta-study demonstrated that ZERODUR is much more resistant with respect to radioactive environment than thought before. Investigations on this topic continues [1/5/45, 49].
- Research on mechanical strength of ZERODUR proves the existence of a threshold stress for a given surface condition below which no residual statistical breakage risks exist. This allows applying ZERODUR at considerably higher stress loads than thought before. A verified model allows calculating the minimum lifetime for a given stress including the fatigue caused by environmental humidity [2/4/24, 25].
- Progress in CNC grinding makes highly lightweighted mirrors possible with large diameters. A 1.2-m demonstrator mirror exists and has been thoroughly tested. A study confirms the feasibility of 4-m diameter highly lightweighted mirrors [2/6/40, 41, 45].
- 4-m mirror blanks can be ground to off-axis aspherical shape with lower double digit micrometer tolerances reducing the finishing time for the mirror significantly [2/6.4/41, 47].

Even though these improvements mark a very high level of achievements, this does not mean that there is an end to the developments for ZERODUR. From its very beginning throughout its whole history, this material has followed demands and requirements getting more and more challenging. There is reason to be optimistic also for the future.

Acknowledgments

The authors would like to thank all users of ZERODUR for their open and constructive feedback and their continuous challenging of the material's quality and properties, the company Schott's production capabilities and capacities. This is the main driver behind the astonishing development the material has taken in the last two decades. We also thank the many colleagues at Schott, who were the ones making it possible by courageous decisions, ingenious modeling, metrology and engineering, outstanding craftsmanship, and maintaining close communication with the users. We also would like to thank especially Dietrich Lemke of the Max-Planck-Institute for Astronomy in Heidelberg Germany for initiating this article.

References

1. H. Bach, Ed., *Low Thermal Expansion Glass Ceramics*, Springer Science & Business Media (2013).
2. T. Döhring et al., "Forty years of ZERODUR® mirror substrates for astronomy: review and outlook," *Proc. SPIE* **7018**, 70183B (2008).
3. T. Döhring et al., "Heritage of ZERODUR® glass ceramic for space applications" *Proc. SPIE* **7425**, 74250L (2009).
4. R. Jedamzik et al., "Homogeneity of the coefficient of linear thermal expansion of ZEDRODUR," *Proc. SPIE* **5868**, 58680S (2005).
5. R. Jedamzik, R. Müller, and P. Hartmann, "Homogeneity of the linear thermal expansion coefficient of ZERODUR® measured with improved accuracy," *Proc. SPIE* **6273**, 627306 (2006).
6. P. Hartmann et al., "Glass ceramic: even closer to zero thermal expansion: a review, part 1," submitted to *J. Astron. Telesc. Instrum. Syst.* (2021).
7. R. Jedamzik, T. Werner, and T. Westerhoff, "Production of the 4.26 m ZERODUR® mirror blank for the Advanced Technology Solar telescope (ATST)," *Proc. SPIE* **9151**, 915131 (2014).
8. R. Jedamzik, C. Kunisch, and T. Westerhoff, "Effects of thermal inhomogeneity on 4m class mirror substrates," *Proc. SPIE* **9912**, 99120Z (2016).
9. R. Jedamzik and T. Westerhoff, "Homogeneity of the coefficient of linear thermal expansion of ZERODUR®: a review of a decade of evaluations," *Proc. SPIE* **10401**, 104010J (2017).
10. R. Jedamzik, P. Hartmann, and T. Westerhoff, "CTE homogeneity of ZERODUR® in the ELT century," *Proc. SPIE* **11451**, 114511B (2020).
11. R. Jedamzik et al., "CTE characterization of ZERODUR® for the ELT century," *Proc. SPIE* **7425**, 742504 (2009).
12. R. Jedamzik et al., "Glass ceramic ZERODUR® enabling nanometer precision," *Proc. SPIE* **9052**, 90522I (2014).
13. R. Jedamzik, C. Kunisch, and T. Westerhoff, "ZERODUR® thermo-mechanical modelling and advanced dilatometry for the ELT generation," *Proc. SPIE* **9912**, 99120J (2016).
14. H. F. Morian, K. Knapp, and P. Hartmann, "Quality-assurance demands and realization for thin-walled mirror blanks made of ZERODUR® for the AXAF project," *Proc. SPIE* **1993**, 1–12 (1993).
15. T. Doehring et al., "Production of the 4.1-m Zerodur mirror blank for the VISTA Telescope," *Proc. SPIE* **5494**, 340–349 (2004).
16. T. Westerhoff et al., "Progress in 4 m class ZERODUR mirror production," *Proc. SPIE* **8126**, 81260A (2011).
17. R. Jedamzik and P. Hartmann, "Influence of striae on the homogeneity of the linear thermal expansion coefficient of ZERODUR®," *Proc. SPIE* **6288**, 62880M (2006).
18. T. Westerhoff et al., "Performance of industrial scale production of ZERODUR® mirrors with diameter of 1.5 m proves readiness for the ELT M1 segments," *Proc. SPIE* **8444**, 844437 (2012).
19. E. Werner, "Zur Bestimmung der Spannungsdoppelbrechung von optischem Glas," *Silikattechnik* **18**, 45–49 (1967).

20. "ISO 11455:1995 raw optical glass—determination of birefringence," International Organization for Standardization, Geneva (1995).
21. H. Katte, "Measuring of high quality optics for lithography: fast and high-resolution measurement of stress birefringence in large-format optical materials," *Opt. Photonik* **4**(2), 26–29 (2009).
22. W. Weibull, "A statistical distribution function of wide applicability," *ASME J. Appl. Mech.* **18**(3), 293–297 (1951).
23. P. Hartmann, "ZERODUR® Strength modelling with Weibull statistical distributions," *Proc. SPIE* **9912**, 991208 (2016).
24. P. Hartmann, "ZERODUR®: deterministic approach for strength design," *Opt. Eng.* **51**(12), 124002 (2012).
25. P. Hartmann, "Minimum lifetime of ZERODUR® structures based on the breakage stress threshold model: a review," *Opt. Eng.* **58**(2), 020902 (2019).
26. S. W. Freiman, S. M. Wiederhorn, and J.J. Mecholsky, "Environmentally enhanced fracture of glass: a historical perspective," *J. Am. Ceram. Soc.* **92**(7), 1371 (2009).
27. M. Ciccotti, "Stress-corrosion mechanisms in silicate glasses," *J. Phys. D: Appl. Phys.* **42**, 214006 (2009).
28. T. Westerhoff, T. B. Hull, and R. Jedamzik, "ZERODUR manufacturing capacity: ELT and more," *Proc. SPIE* **11116**, 1111612 (2020)
29. H. F. Morian and R. H. Mauch, "ZERODUR® for lightweight secondary/tertiary mirrors," *Proc. SPIE* **3352**, 140–150 (1998).
30. E.-D. Knohl, A. Schoeppach, and M. A. Pickering, "Status of the secondary mirrors (M2) for the Gemini 8-m telescopes," *Proc. SPIE* **3352**, 258–267 (1998).
31. T. Döhring et al., "Manufacturing of lightweighted ZERODUR® components at Schott," *Proc. SPIE* **6666**, 666602 (2007).
32. T. Westerhoff et al., "Manufacturing of the ZERODUR® 1.5-m primary mirror for the solar telescope GREGOR as preparation of light weighting of blanks up to 4-m diameter," *Proc. SPIE* **7739**, 77390M (2010).
33. T. Hull et al., "Game-changing approaches to affordable advanced lightweight mirrors: extreme Zerodur® lightweighting and relief from the classical polishing parameter constraint," *Proc. SPIE* **8125**, 81250U (2011).
34. T. Westerhoff et al., "Lightweighted ZERODUR® for telescopes," *Proc. SPIE* **9151**, 91510R (2014).
35. T. E. Brooks et al., "Modeling the extremely lightweight Zerodur® mirror (ELZM) thermal soak test," *Proc. SPIE* **10374**, 103740E (2017).
36. T. E. Brooks, R. Eng, and H. P. Stahl, "Optothermal stability of large ULE and Zerodur mirrors," *Proc. SPIE* **10743**, 107430A (2018).
37. A. Leys, T. Hull, and T. Westerhoff, "Cost-optimized methods extending the solution space of lightweight spaceborne monolithic ZERODUR® mirrors to larger sizes," *Proc. SPIE* **9573**, 95730E (2015).
38. A. Leys, T. Hull, and T. Westerhoff, "Production of ELZM mirrors: performance coupled with attractive schedule, cost, and risk factors," *Proc. SPIE* **9911**, 99112P (2016).
39. T. Hull, T. Westerhoff, and R. Jedamzik, "Optimizing ZERODUR mirror substrate fabrication processes for efficient optical fabrication," *Proc. SPIE* **11116**, 1111615 (2020).
40. T. Westerhoff, T. B. Hull, and R. Jedamzik, "Establishing a substrate manufacturing center for ZERODUR 4-meter diameter lightweight mirrors," *Proc. SPIE* **11117**, 1111706 (2020).
41. H. P. Stahl, "Overview and performance prediction of the baseline 4-meter telescope concept design for the habitable-zone exoplanet observatory," *Proc. SPIE* **10698**, 106980W (2018).
42. T. Hull et al., "Use of updated material properties in parametric optimization of spaceborne mirrors," *Proc. SPIE* **9904**, 99046B (2016).
43. T. Hull, A. Carre, and R. Jedamzik, "ZERODUR as a dimensionally stable mirror substrate material for spaceborne telescopes," *Proc. SPIE* **11180**, 1118017 (2019).
44. T. Hull et al., "Practical aspects of specification of extreme lightweight Zerodur® mirrors for spaceborne missions," *Proc. SPIE* **8836**, 883607 (2013).

45. A. Hull and T. Westerhoff, "Lightweight Zerodur®: optimized athermal performance for Space Telescopes," in *Am. Astron. Soc. Meeting Abstracts #231* (2018).

Peter Hartmann received his doctorate degree in physics from the University of Mainz, Mainz, Germany, in 1984. From 1985 to 2018, he has held different positions at Advanced Optics of Schott AG Mainz. He served on the SPIE Board of Directors from 2011 to 2013, the Board of Trustees of the Max-Planck-Institute for Astronomy, Heidelberg, Germany, and as a convener of ISO and DIN working groups. He is a fellow of SPIE and a senior member of OSA.

Ralf Jedamzik received his diploma degree in physics from the University of Düsseldorf and his doctorate degree in material science from the Technical University Darmstadt. In 1999, he joined Schott as a quality technology expert. Since 2013, he has been a principal scientist and a leader of ZERODUR® and optical glass development projects. As an application manager, he works as an international technical consultant for numerous industrial projects. He has authored more than 50 papers and is a senior member of the SPIE.

Antoine Carré has graduated as a chemical engineer and theoretical chemical physicist. He obtained his international PhD in theoretical chemistry related to the atomistic description of glass material. Since 2010, he has been belonging to the Development Department of the Optical Business Unit of the Glass Manufacturer Schott. His main focus areas are process optimization, support to production, and material properties investigation under extreme conditions.

Janina Krieg received her master's degree in physics from the University of Stuttgart, Stuttgart, Germany, and her doctorate degree in material science from the Technical University of Darmstadt, Darmstadt, Germany, in 2017. In the same year, she joined the Advanced Optics Unit of Schott AG, Mainz, Germany. She is the responsible product manager for ZERODUR® glass ceramics for aerospace applications.

Thomas Westerhoff received his doctorate degree in physics from the University of Mainz. He joined the Optics Business at Schott as a product manager in 1996. He was promoted to director of sales and marketing Schott Lithotec in 1999. In 2007, he took responsibility for the Schott Product Group ZERODUR®. In 2018, he was promoted to the position vice president Strategic Business Field ZERODUR® responsible for astronomy and space, IC and FPD lithography, and industrial application.